Proceedings of the IV Forum EMR–PL, June 27–29, 2016, Poznań, Poland

EPR and Impedance Measurements of Graphene Oxide and Reduced Graphene Oxide

M. Kempiński[a,b,*], S. Łoś[c], P. Florczak[b], W. Kempiński[c] and S. Jurga[a,b]

[a]Faculty of Physics, Adam Mickiewicz University, Umultowska 85, 61-614 Poznań, Poland

[b]NanoBioMedical Centre, Adam Mickiewicz University, Umultowska 85, 61-614 Poznań, Poland

[c]Institute of Molecular Physics, Polish Academy of Sciences, M. Smoluchowskiego 17, 60-179 Poznań, Poland

We report the observations of electron paramagnetic resonance and impedance measurements of graphene oxide and reduced graphene oxide performed in the wide temperature range in order to get insight into the electronic properties of graphene-based materials and the role of oxygen functionalities in the charge carrier transport phenomena. In such systems the strong spin localization, hopping charge carrier transport as well as the formation of adsorption layers are observed, all the phenomena changing significantly after the heavily oxidized graphene is reduced.

DOI: 10.12693/APhysPolA.132.81

PACS/topics: 72.80.Vp, 76.30.–v

1. Introduction

Graphene-based materials are among the most popular systems in the solid state science recently. It is mostly due to their peculiar electronic properties, which are considered very promising from the point of view of many applications in electronics, spintronics, photovoltaics, energy storage, etc. Especially interesting is the fact that the pure graphene layer shows ballistic conduction [1], while introduction of defects causes the strong electron localization, which can even lead to the magnetism of graphene-based materials [2]. The main source of defects is obviously the edge of a layer, with the zig-zag conformation generating the localized states [3, 4]. Other atoms can attach to the graphene layer only at the defects, because the in-plane C–C bonds (σ bonds) are very strong and chemically inert. It is very common that graphene-based materials contain a lot of oxygen functional groups at the surface [5] and it seems that these groups are responsible for the good adsorption properties of active carbons. This is especially important in case of adsorption of water and other species containing the –OH groups, as pure graphene is strongly hydrophobic [6]. We have already shown that the adsorption of molecules in the active carbons significantly influences their electronic properties, having big impact on the localization of the charge carriers within their structure [7–9]. Charge carrier localization effects produce paramagnetic centers, which can be well observed using the electron paramagnetic resonance (EPR).

Another effect of the oxidation of graphene is the increase of the material's resistivity by several orders of magnitude, turning it from the conductor to the insulator. Thus, coupling the EPR with electric transport measurements should allow to trace changes of electronic properties caused by oxidation or reduction of graphene layers and also to observe the influence of this processes on the adsorption properties of the material. The AC impedance measurements, besides looking at the resistivity of the material, should give some insight into the effects occurring at the grain boundaries, where two grains are considered to form an electrical capacitor [10]. This problem is very important from the point of view of sophisticated applications of the systems where the conducting nano-elements are separated by potential barriers for charge transport. It was shown for very pure graphene-based material that it is possible to control its conducting properties via controlling the stress level which directly influences the conditions of electrical connections between the graphene plates [11]. Even very slight stress change, e.g. due to the flow of blood in veins can be detected by measuring the electrical conduction of the graphene-based sensor [12]. This problem is very close to our previous work on the control of conducting properties via modifications of connections between the graphite-like nanoparticles in ACFs [7, 9].

It is known that ACFs comprise small graphene fragments with addition of oxygen functional groups, thus should show some similarities with another graphene-based materials. In this work we attempt to compare the localization processes in the graphene oxide (GO) and reduced graphene oxide (RGO) with conditions at the boundary grains which allow to control carrier transport in ACFs. Measurements were performed in the wide temperature range and are devoted to describe localization processes studied by EPR and AC impedance methods.

2. Experimental

GO sample was obtained from the graphite powder using the modified Hummers method [13]. This method utilizes the mixture of $NaNO_3$, H_2SO_4 and $KMnO_4$ to introduce oxygen into the graphite crystal lattice, and subsequent washing with deionized water and ultrasonication which results in the exfoliation of the graphene

*corresponding author; e-mail: matt@amu.edu.pl

layers [14]. The obtained material consists of highly oxidized single- and multilayer graphene, with no residuals from the chemical treatment.

RGO was prepared from the GO material by reduction with hydrazine monohydrate.

EPR measurements were performed using the Radiopan ES/X spectrometer equipped with the Oxford Instruments gas flow helium cryostat (1.5 ÷300 K). Samples were placed in the quartz tubes in the ambient condition and sealed with parafilm.

For the impedance measurements, powdered RGO sample was placed inside the cylindrical capacitor, while the rigid thin flake of GO got electrodes glued directly to it with the use of the silver paste. The thickness of the sample was about 0.1 mm. Helium was used as the medium for heat transfer from the sample. Impedance was measured with the Agilent E 4980 RLC bridge in the frequency range of $20 \div 2 \times 10^6$ Hz and temperature in the $4.2 \div 300$ K range.

3. Results and discussion

EPR signal of GO is well observed in room temperature (RT) and it consists of two narrow Lorentzian lines with g-factor values characteristic of carbon materials. The EPR spectrum is presented in Fig. 1 and the line parameters in Table I. The signal linewidth and amplitude evolve with temperature. Linewidth increases with the temperature lowering by the factor of 2, while amplitude significantly decreases when cooling down to 100 K, and increases below 100 K. The integral intensities of both lines increase when temperature decreases, but neither of them follows the Curie law, as would be for pure Langevin paramagnetism.

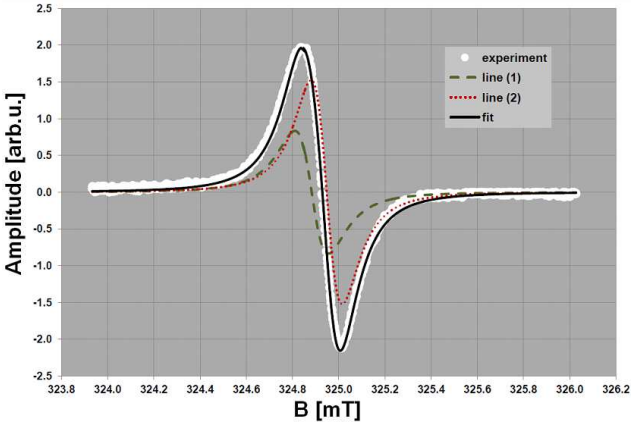

Fig. 1. EPR spectrum of GO at RT. Spectrum deconvolution shows two component lines.

EPR signal of RGO can be observed only below 100 K and the correct deconvolution is possible for signals recorded in temperatures below 50 K (due to poor signal-to-noise ratio in higher T-range). According to the "granular metal" model, which was successfully used for ACF [7], as the temperature increases, the thermal excitations allow charge carriers hopping over the potential barriers in the system. Thus less spins are localized and EPR signal vanishes. Similar situation occurs in RGO.

TABLE I

Line parameters ΔB [mT] and g of all the components extracted from the EPR spectra of GO and RGO.

Sample	Line (1)		Line (2)		Line (3)	
	ΔB	g	ΔB	g	ΔB	g
GO (RT)	0.13	2.0031	0.12	2.0027	–	–
GO (LT)	0.28	2.0032	0.27	2.0026	–	–
RGO (LT)	0.42	2.0031	1.36	2.0026	6.49	2.0038

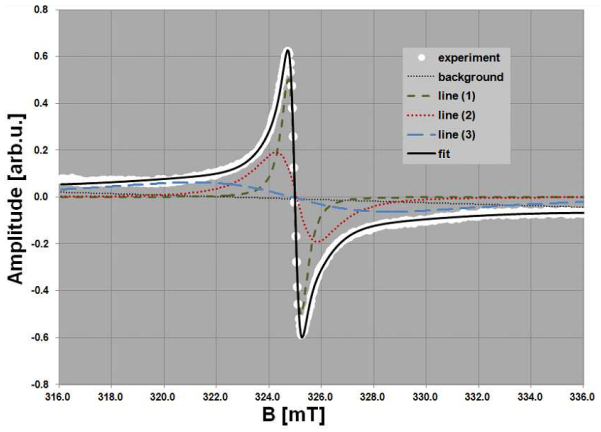

Fig. 2. EPR spectrum of RGO at 4 K. Spectrum deconvolution shows three component lines.

The EPR spectrum of RGO is presented in Fig. 2 and its parameters in Table I. The spectrum consists of three component lines, where g-factor values of line (1) and (2) are constant regardless of temperature, g-factor of the line (3) decreases with increase of temperature. Linewidths of all components are constant and integral intensities of all three lines show the Curie-like characteristics.

In our previous works concerning activated carbon fibers [2, 3] and active carbon materials [15] EPR signals were almost the same as observed for RGO, with similar g values and temperature evolution. Three signals were ascribed to the three different paramagnetic centers:
— line (1) from "pure" carbon (not in contact with adsorbed molecules),
— line (2) from carbon interacting with molecules adsorbed at adsorption sites where adsorbed molecules get strongly immobilized at the surface,
— line (3) from carbon at adsorption sites where adsorbed molecules show more "freedom" of rotational movements.

The behaviour of the three components of the EPR signal of RGO seems to fit this description.

GO shows two signals with the same g-factor values as RGO, thus we can assume that these lines origin from the

paramagnetic centers of the same type. Both lines show smaller linewidth and line (2) is even narrower than the line (1) which is much different from the RGO. As it was mentioned above the line (1) is related to spins localized at the "pure" carbon, the line (2) originates from the spins strongly interacting with molecules adsorbed at the carbon surface. It is the most probable that places where oxygen groups are attached to the graphene are the preferential adsorption sites. As there are much more such sites in GO than in RGO and ACF due to heavy oxidation, there should also be more spins and the exchange interaction could take place, narrowing the EPR signal.

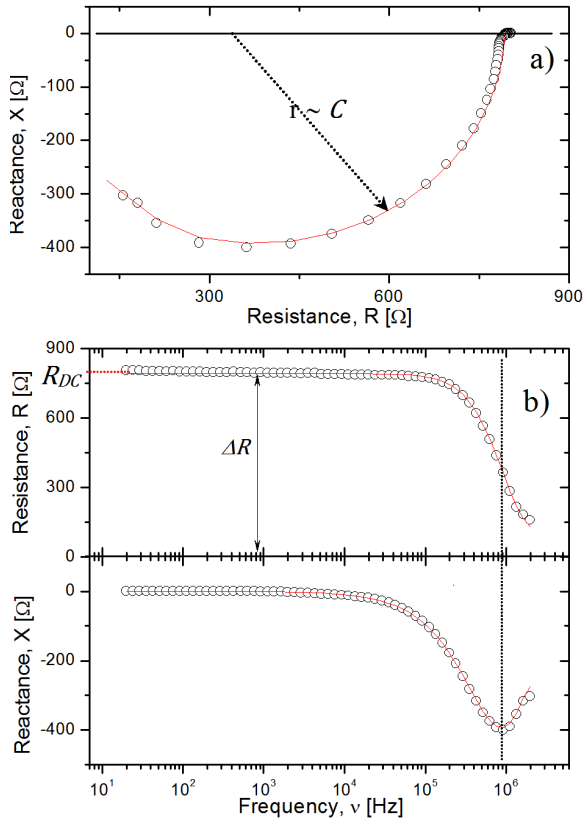

Fig. 3. The Nyquist plot of RGO sample at 42 K (a) and the impedance spectra (b). The solid line represents the best fit to experimental points of Eq. (1).

Impedance measurements show that regardless of the sample shape the main mechanism responsible for the electric current flow is the charge hopping between the grains. This problem is discussed in paper [16] where increase of conductivity with decrease of temperature is observed. Hopping was also observed in our experiments and occurs with the characteristic time constant τ which cause a phase shift between the applied transport voltage and the flowing current. For the frequencies lower than the reciprocal value of τ the sample possesses resistive character — see Fig. 3b. For higher frequencies the charge movement is limited only to the grain dimension and no energy loss is observed, thus the measured resistance value decreases. Obtained results can be analyzed in the Nyquist plot Fig. 3a which is a complex plane of measured reactance (imaginary part) and resistance (real part). Each frequency point at the certain temperature fulfils the impedance relation

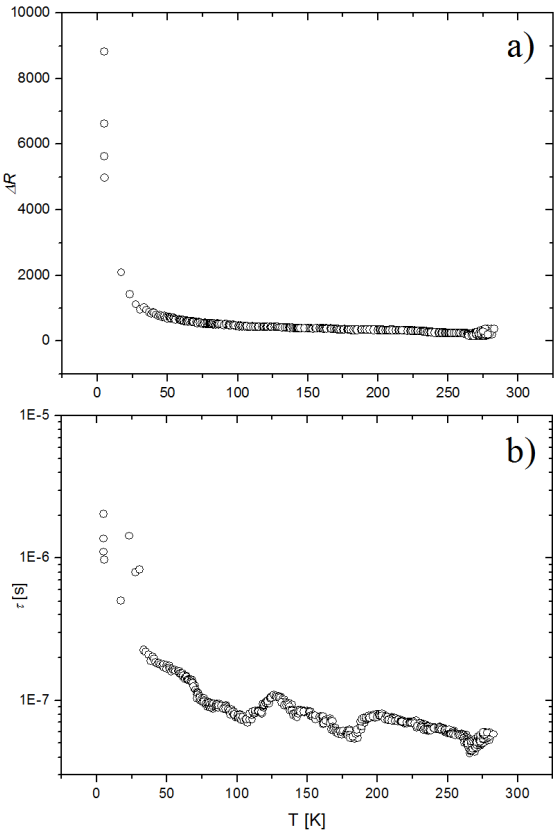

Fig. 4. The temperature dependence of ΔR and τ parameters for RGO sample, respectively (a) and (b). These values were obtained from fitting procedure of Eq. (1).

$$Z = \frac{\Delta R}{1 + \omega\tau i}, \tag{1}$$

where ΔR — resistance step, ω — frequency of the applied electric field and τ — characteristic time for the charge carrier jump. Solution of this equation forms the characteristic semicircle on the Nyquist plot. A cross point with the real axis, obtained from extrapolation of low-frequency impedance, represents the highest resistivity equivalent to the DC measurements. As the flowing current outruns the applied voltage the reactance value goes below zero due to the sample capacitance, C influencing the semicircle radius. C value can be easily obtained from the relation of $\Delta RC = \tau$. The main reason for the capacitance appearing is the delay in the charge jump. The τ parameter impacts the minimum reactance and is the reciprocal value of the specified frequency. Due to the adsorption phenomena an interface forms between the graphenes and it can be expected that the impedance will be composed of the three character-

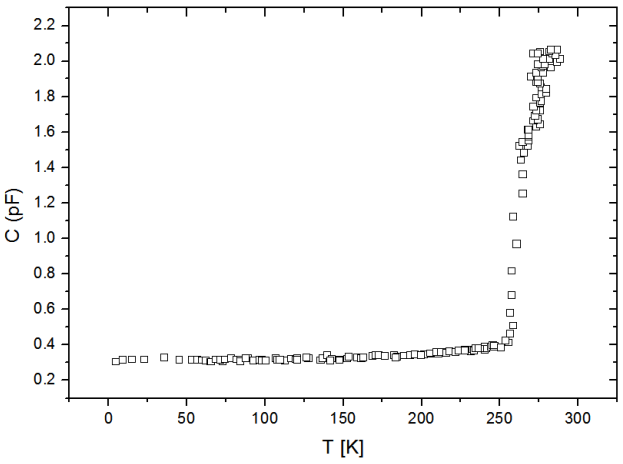

Fig. 5. The capacity of GO sample calculated from reactance for frequency of 928 Hz plot versus temperature.

istic semicircles [17]. Two of them will represent charges forming a classical double electric layer [18, 19]. Charge accumulated on the solid phase of the interface creates the depletion layer with ions kept on opposite sides by the Coulomb interactions. The third semicircle represents processes occurring on the most outer layer of the system, where slow diffusive exchange can occur. This surface is known as the Gouy–Chapman layer. Such three-layer system is very sensitive, which can be observed by measuring the following parameters: R_{DC}, ΔR, C and τ. Each layer responses with different τ value to the change of the applied electric field. The shortest response time characterizes charges with the highest mobility. Without doubt these are carriers collected in the depletion layer at the solid phase. The hopping process taking place inside the ion layer is slower as it involves reorientation of the larger mass. The longest τ value will be observed for diffusion phenomena.

Impedance measurements of both samples studied show only one semicircle with rather short τ — hundreds of nanosecond, see Fig. 4. This value points at the high mobility and it has to be assigned to depletion layer. In this case, there would be no difference between R_{DC} and ΔR.

The charge hopping is activated by thermal energy. Its lowering results in the increase of τ and ΔR. For RGO sample the temperature dependence of measured parameters is presented in Fig. 4. The GO sample produced with the modified Hummers method is a poor conductor, which is reflected by ΔR equal to 5 MΩ at room temperature. In contrast, the value registered for RGO equals 80 Ω. Decrease of the temperature causes the increase of this parameter up to the hundreds of GΩ at 4.2 K for GO. Due to the long τ this material behaves as a classical dielectric. The strong localization phenomena are observed for both samples but on account of low doping (resulting from adsorption) it has a powerful impact on GO. A mutual relation between capacitance of both samples is about 200. This difference is caused by dissimilarity of the ΔR parameter ($C = \tau/\Delta R$). The capacitance versus temperature for GO sample is shown in Fig. 5. Sudden decrease at 260 K suggests that the charge forming the depletion layer can come from adsorbed water molecules. As both materials show weak adsorption properties due to poorly developed porosity, the capacitance of samples is small as well.

4. Conclusions

Presented experiments lead us to the following conclusions:

- GO shows EPR signal in RT, its amplitude decreases until 100 K and then increases. Linewidth increases with the T decrease in the whole T range, giving monotonic increase of integral intensity (non-Curie). The non-Curie behaviour suggests the existence of mixed localized and delocalized paramagnetic centres. Narrowing of the EPR signal of GO might be connected with the different relaxation times or with the exchange interaction.

- RGO shows the EPR signal only below 100 K — in the range where both ΔR and τ parameters observed in the impedance measurements monotonically increase. This correlation clearly shows that below 100 K electrical transport between the graphene layers becomes suppressed as the charge carriers become localized and "stored" in the local capacitors formed by the graphene layers.

- Due to faint porosity the measured capacitance is rather small for both samples. The impedance measurement reveal only one semicircle as accumulated charges form depletion layer with characteristic short τ value.

- RGO shows much higher density of delocalized charge than GO. The impedance module for RGO is lower than that of GO by almost 5 orders of magnitude at room temperature. This might be due to the strong localization of the charge carriers at the defects in graphene layers terminated with oxygen functionalities.

- For both samples at temperature about 260 K are seen capacitance changes. This might suggest that conducting properties are stimulated by the small amount of water molecules adsorbed at the graphene surface. The molecules could act as donors or acceptors of charge in the system.

- Below 40 K strong adsorption of helium might occur (which is a common phenomenon in carbon systems, known as the sorption pump) causing a large increase of the characteristic time τ of the RGO.

All the above results show the fundamental electronic differences between GO and RGO. Oxygen functional groups located at the edges and defects play the crucial role in the system of graphene layers, which can be considered as separate small conducting objects. These functionalities strongly affect the potential barriers between the graphenes, which are responsible for localization of spins observed with EPR. Impedance measurements allowed us to propose the capacitor model for localization phenomena, where charge carriers get stored (localized) at the local capacitors formed between the graphenes inside the examined material. This method gives several parameters like: R_{DC}, ΔR, C, and τ to perform control on the connection properties.

Acknowledgments

This work was partially supported by the National Center of Science, Grants Nos. DEC-2013/09/B/ST4/03711 and DEC-2014/15/B/ST3/02927.

References

[1] K.S. Novoselov, A.K. Geim, S.V. Morozov, D. Jiang, Y. Zhang, S.V. Dubonos, I.V. Grigorieva, A.A. Firsov, *Science* **306**, 666 (2004).

[2] Ł. Majchrzycki, M.A. Augustyniak-Jabłokow, R. Strzelczyk, M. Maćkowiak, *Acta Phys. Pol. A* **127**, 540 (2015).

[3] V.L.J. Joly, K. Takahara, K. Takai, K. Sugihara, T. Enoki, M. Koshino, H. Tanaka, *Phys. Rev. B* **81**, 115408 (2010).

[4] M.A. Augustyniak-Jabłokow, M. Maćkowiak, K. Tadyszak, R. Strzelczyk, *Acta Phys. Pol. A* **127**, 537 (2015).

[5] J.K. Brennan, T.J. Bandosz, K.T. Thomson, K.E. Gubbins, *Coll. Surf. A* **187-188**, 539 (2001).

[6] H. Sato, N. Kawatsu, T. Enoki, M. Endo, R. Kobori, S. Maruyama, K. Kaneko, *Carbon* **45**, 214 (2007).

[7] M. Kempiński, W. Kempiński, J. Kaszyński, M. Śliwińska-Bartkowiak, *Appl. Phys. Lett.* **88**, 143103 (2006).

[8] M. Kempiński, M. Śliwinska-Bartkowiak, W. Kempiński, *Rev. Adv. Mater. Sci.* **14**, 163 (2007).

[9] W. Kempiński, D. Markowski, M. Kempiński, M. Śliwińska-Bartkowiak, *Carbon* **57**, 533 (2013).

[10] B. Abeles, P. Sheng, M.D. Coutts, Y. Arie, *Adv. Phys.* **24**, 407 (1975).

[11] K.R. Paton, E. Varrla, C. Backes, R.J. Smith, U. Khan, A. O'Neill, C. Boland, M. Lotya, O.M. Istrate, P.King, T. Higgins, S. Barwich, P. May, P. Puczkarski, I. Ahmed, M. Moebius, H. Pettersson, E. Long, J. Coelho, S.E. O'Brien, E.K. McGuire, B. Mendoza Sanchez, G.S. Duesberg, N. McEvoy, T.J. Pennycook, C. Downing, A. Crossley, V. Nicolosi, J.N. Coleman, *Nat. Mater.* **13**, 624 (2014).

[12] C.S. Boland, U. Khan, G. Ryan, S. Barwich, R. Charifou, A. Harvey, C. Backes, Z. Li, M.S. Ferreira, M.E. Möbius, R.J. Young, J.N. Coleman, *Science* **354**, 1257 (2016).

[13] W.S. Hummers Jr., R.E. Offeman, *J. Am. Chem. Soc.* **80**, 1339 (1958).

[14] S. Łoś, L. Duclaux, L. Alvarez, Ł. Hawełek, S. Duber, W. Kempiński, *Carbon* **55**, 53 (2013).

[15] S. Łoś, L. Duclaux, W. Kempiński, M. Połomska, *Micropor. Mesopor. Mater.* **130**, 21 (2010).

[16] X.Y. Huang, C. Zhi, P.K. Jiang, D. Golberg, Y. Bando, T. Tanaka, *Nanotechnology* **23**, 455705 (2012).

[17] Z. Hens, W.P. Gomes, *J. Phys. Chem. B* **103**, 130 (1999).

[18] C.-T. Hsieh, H. Teng, *Carbon* **40**, 667 (2002).

[19] J. Biener, M. Stadermann, M. Suss, M.A. Worsley, M.M. Biener, K.A. Rose, T.F. Baumann, *Energy Environ. Sci.* **4**, 656 (2011).